International Journal on
"Technical and Physical Problems of Engineering"
(IJTPE)
Published by International Organization of IOTPE

ISSN 2077-3528
IJTPE Journal
www.iotpe.com
ijtpe@iotpe.com

June 2014 | Issue 19 | Volume 6 | Number 2 | Pages 138-144

MODELING AND CONTROL OF ASYMMETRIC Γ-SOURCE INVERTERS FOR PHOTOVOLTAIC APPLICATIONS

F. Khoshkhati [1] S. Toofan [2] B. Asaei [1]

1. Department of Electrical and computer Engineering, University of Tehran, Tehran, Iran
f.khoshkhati@gmail.com, b.asaei@ut.ac.ir
2. Department of Electrical and computer Engineering, University of Zanjan, Zanjan, Iran, s.toofan@znu.ac.ir

Abstract- This paper presents a power electronic interface converter based on asymmetric Γ-Source Inverter for photovoltaic application. The average state space model of the system is used for modeling of the proposed converter system. According to the obtained model of system, a two stage controller is designed to regulate the capacitor voltage of the impedance network to its required voltage and regulate Photovoltaic system voltage to its reference provided in maximum power point algorithm. To this aim, inverter modulation index, which is produced in AC side current controller, is used to adjust capacitor voltage in impedance network and inverter shoot through duty cycle is used to regulate PV voltage to its reference. Performance of the proposed two stage controller is verified using simulation in MATLAB/Simulink.

Keywords: Power Electronic Interface, Asymmetrical Γ-Source Inverter, Photovoltaic.

I. INTRODUCTION

In recent years, Photovoltaic (PV) systems have become one of the most important renewable energy resources (RERs). Noiseless operation, low maintenance requirement and generating power from free source of sun make PV systems more popular among other RERs. Since source of PV system is free, its major cost is its installation cost, which is mainly composed the cost of PV module and power electronic interface (PEI) system. By the development of solar cell technology, manufacturers are able to produce solar cells with lower prices.

Despite the reduction of cost in solar cells, the PEI systems price is rather the same. Therefore, to reduce the installation cost of PV system, this is necessary to reduce PEI cost. Voltage source inverters (VSIs) are most popular converter for converting DC power to AC in PV applications. This inverter is only a buck inverter from DC side to AC side, therefore in those applications that need boost capability, an additional DC/DC converter is used. Utilizing an excessive converter stage increases cost, volume and losses of total PEI system.

Z-source inverter (ZSI) proposed in [1] is a buck-boost single stage PEI system. Unlike VSI, utilizing an impedance network between DC source and inverter legs and dedicating inverter shoot through cycles in ZSI switching algorithm, which is unallowable in VSI, the DC source voltage, can be boosted to a higher level without any extra converter stages. This unique feature of the ZSI makes it a suitable PEI system for many applications such as fuel cells, RERs, uninterruptible power supplies and power quality improvements [2-8].

According to the single stage power conversion of ZSI, for proper operation of ZSI pulse width modulation (PWM), the inverter shoot through duty cycle (D) and inverter modulation index (M) is related to each other and confined each other's to an upper level. Achieving boost capability with higher D leads to reduction of M, which increases voltage stress on inverter switches. Therefore, this is necessary to achieve boost capability with higher M and lower D. To this aim maximum boost and maximum constant boost control strategy based on ZSI switching algorithm is proposed to lower the voltage stress on switches [9, 10].

Addition to the switching control strategy, some more advanced type of ZSI is proposed in literatures to achieve higher voltage gain in lower D to reduce voltage stress on switches in inverter legs. Switched Z-Source inverter utilizes six extra diodes in impedance network to achieve more voltage boost capability [11]. Utilizing a high frequency transformer in impedance network, trans-Z-source inverter can have more voltage gain than traditional ZSI when the transformer turn ratio is increased [12]. T-Z-source inverter utilizes two transformers in its impedance network to increase the boost capability of the inverter [13].

In high frequency transformer based Z-source inverters, for achieving more boost capability, it is required to increase the turn ratio of the transformer. Increase in turn ratio of transformer leads to need for higher transformer winding and higher current stress on the legs which are in shoot through state. To cope with the problem one can resort to asymmetric Γ-source inverter proposed in [14]. In this converter structure, the voltage gain of the converter increases when turn ratio of transformer is reduced. Having lower transformer turn ratio with higher boost capability reduces the volume of windings and voltage and current stress on inverter switches.

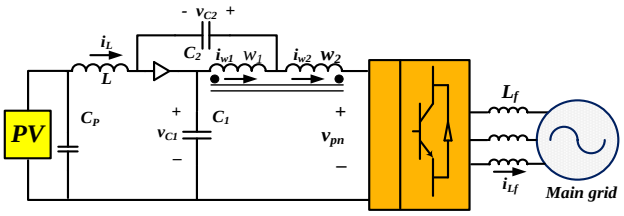

Figure 1. The proposed PEI system

Moreover, in this structure of impedance network, the DC source is serried with an inductor, which reduces high frequency ripples on DC source current and eliminates the need of excessive large filters in DC source. Interesting to advantages of Γ-source inverter, in this paper this type of inverter is used as a PEI system for photovoltaic applications. To this aim, a two stage controller is presented to regulate capacitor voltage of the impedance network to its reference and regulate PV voltage to the reference voltage provided in maximum power point tracking algorithm [15].

In this control manner, the capacitor voltage is set to its reference using inverter modulation index so that the PWM algorithm is properly operated and keeps balance between PV power producing and injected power to grid. The average state space method is used for modeling and design of the capacitor voltage controller. After design of capacitor voltage controller in a certain bandwidth, the PV voltage controller, which set the PV voltage to its reference using inverter shoot through duty cycle is designed with a bandwidth lower than capacitor voltage controller.

This paper is organized as follows, in section II, the asymmetrical Γ-source inverter is modeled by average state space model. In section III, the two stages control strategy is presented and the controller coefficients are obtained according to the system model in section II. Performance of the proposed controller is evaluated using simulation in MATLAB/Simulink.

II. MODELING OF ASYMMETRICAL Γ-SOURCE INVERTER

The PV system based on asymmetrical Γ-source inverter as PEI system is shown in Figure 1. As can be seen, the power conversion process in this converter is single stage without any excessive DC/DC converter. In this configuration, a high frequency transformer is utilized to increase boost capability of the converter. To investigate the operation of the PEI system, its equivalent circuit in shoot through and nonshoot through states are shown in Figure 2(a) and (b) respectively.

In this figure, the absorbed current from impedance network is modeled by current source of i_o while switch S represents the switching state of inverter legs. In shoot through state, the switch S is turned on and make the end of the impedance network short circuited. In this interval, the diode *D* is reverse biased. During this condition, the DC source energy and the electrostatic energy stored in capacitors are released in inductors and stores in them magnetically. In nonshoot through state, switch S is turned off and output current is supplied by impedance network.

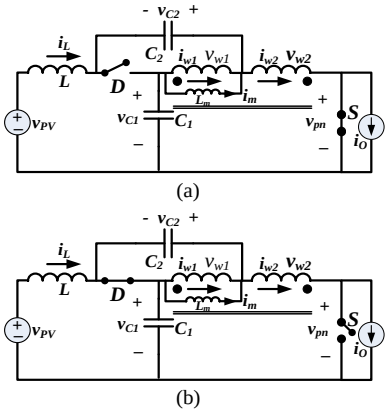

Figure 2. Equivalent circuit of PEI system, (a) in shoot through, (b) in nonshoot through state [14]

In this condition, the diode *D* conducts and energy stored in transformer core and inductor is released to capacitors and increases their voltage level. According Figure 2(a), the corresponding voltages in shoot through is obtained as follows:

$$v_{W1} = v_{W2} + V_{C1} \tag{1}$$

$$v_{W2} + V_{C2} + V_{PV} = v_L \tag{2}$$

$$v_{W1} = n v_{W2} \tag{3}$$

where, n is the transformer turn ratio.

The corresponding voltages in nonshoot through condition is as follows:

$$V_{C1} + v_L = V_{PV}, V_{C2} + v_{W2} + V_{PV} = v_L + v_{pn} \tag{4}$$

$$v_{W1} = -V_{C2}, \quad V_{C1} + v_{W1} + v_{pn} \tag{5}$$

Averaging the voltages across the transformer windings and inductor to zero per switching period and neglecting parasitic resistances then results in [14].

$$V_{C1} = \frac{1-D}{1-(2+\frac{1}{n-1})D} V_{PV} \tag{6}$$

$$V_{C2} = \frac{nD/(n-1)D}{1-(2+\frac{1}{n-1})D} V_{PV} \tag{7}$$

$$V_{pn} = \frac{1}{1-(2+\frac{1}{n-1})D} V_{PV} \tag{8}$$

where, V_{C1}, V_{C2} and V_{pn} represent the capacitor voltage across C_1, C_2 and inverter legs in steady state. The inverter voltage in AC side is as:

$$V_{inv} = M \frac{v_{pn}}{2} \tag{9}$$

According to Equation (8), the boost capability of the asymmetrical Γ-source inverter is increased when the transformer turn ratio is near "1". This means that with a lower transformer windings and volume a high boost capability can be obtained. For dynamic modeling of the impedance network, the average state space method is used. Considering the $x = [i_L\ i_m\ v_{C1}\ v_{C2}]^T$ as state vector of the impedance network, the state space model of the system in Figure 2(a) is as follows:

$$\frac{dx}{dt} = A_{st}x + B_{st}u_0 \tag{10}$$

where,

$$\begin{cases} u_0 = \begin{bmatrix} i_O \\ v_{PV} \end{bmatrix}, \quad B_{st} = \begin{bmatrix} 0 & 1/L \\ 0 & 0 \\ 0 & 0 \\ 0 & 0 \end{bmatrix} \\ A_{st} = \begin{bmatrix} -r_1/L & 0 & 1/(nL-L) & 1/L \\ 0 & 0 & n/(nL_m - L_m) & 0 \\ -1/(nC_1 - C_1) & -n/(nC_1 - C_1) & 0 & 0 \\ -1/C_2 & 0 & 0 & 0 \end{bmatrix} \end{cases} \tag{11}$$

According to Figure 2(b), in nonshoot through state, the space state model of system is as follows:

$$\frac{dx}{dt} = A_{nst}x + B_{nst}u_0 \tag{12}$$

where,

$$\begin{cases} A_{nst} = \begin{bmatrix} -r_1/L & 0 & -1/L & 0 \\ 0 & 0 & 0 & -1/L \\ 1/C_1 & 0 & 0 & 0 \\ 0 & 1/C_1 & 0 & 0 \end{bmatrix} \\ B_{nst} = \begin{bmatrix} 0 & 1/L \\ 0 & 0 \\ -1/C_1 & 0 \\ (1-n)/(nC_1) & 0 \end{bmatrix} \end{cases} \tag{13}$$

Considering Equations (11) and (13), the average state model of the impedance network can be obtained as

$$\frac{dx}{dt} = Ax + Bu_0, \quad y = C_0 x$$

$$\begin{cases} A = DA_{st} + (1-D)A_{nst}, \quad B = DB_{st} + (1-D)B_{nst} \\ C_0 = \begin{bmatrix} 1 & 0 & 0 & 0 \\ 0 & 0 & 1 & 0 \end{bmatrix} \end{cases} \tag{14}$$

To obtain the main transfer functions of the system for design of controllers, the small signal perturbations of $\hat{D}$ and $\hat{i}_o$ are introduced which are small variations of inverter shoot through duty cycle and load current around a given operating point. Considering $\hat{D}$ and $\hat{i}_o$ as inputs, the matrix B_0, and u_0 is changed as:

$$u = \begin{bmatrix} \hat{D} & \hat{i}_o \end{bmatrix}^T$$

$$B = \begin{bmatrix} \frac{nV_{C1}}{L(n-1)} + \frac{V_{C2}}{L} & \frac{nV_{C1}}{L(n-1)} + \frac{V_{C2}}{L} & \frac{-nI_L}{C_1(n-1)} - \frac{nI_{Lm}}{C_1(n-1)} + \frac{I_o}{C_1} & -\frac{I_m}{C_1} + \frac{(n-1)I_o}{nC_1} \\ \frac{-(1-D)}{C_1} & \frac{(1-n)}{nC_1} & 0 & 0 \end{bmatrix} \tag{15}$$

According to Equation (15), the transfer functions that should be used for controller design are as:

$$G_{\hat{i}_o}^{\hat{v}_{C1}} = \frac{\hat{v}_{C1}}{\hat{i}_o} = [0 \quad 0 \quad 1 \quad 0](sI - A)^{-1}B\begin{bmatrix} 0 & 1 \end{bmatrix}^T \tag{16}$$

$$G_{\hat{D}}^{\hat{i}_L} = \frac{\hat{i}_L}{\hat{D}} = [1 \quad 0 \quad 0 \quad 0](sI - A)^{-1}B\begin{bmatrix} 1 & 0 \end{bmatrix}^T \tag{17}$$

III. DISCRIBTION OF THE PROPOSED CONTROL STRATEGY

The proposed two stages control system is shown in Figure 3. As can be seen, the control system is composed of two control systems namely as capacitor voltage controller and PV voltage controller. For design of the total controller, at first the AC side current controller must be designed with a certain bandwidth as inner current controller. At second step, the capacitor voltage controller should be designed as outer controller for AC current controller. In this control method, the capacitor voltage controller provides reference current for AC controller, therefore the AC current controller bandwidth must be higher than capacitor voltage controller. Finally, the PV voltage controller must be designed with bandwidth lower than capacitor controller.

A. AC Side Current Controller

Since the AC current controller is inner controller for other parts of system, it should be designed with a higher bandwidth compare to other parts. As the grid voltage is balanced three phase, utilizing controller in synchronous reference is possible. In synchronous reference frame all variables in AC side is transformed to DC variables, therefore PI controller can be used to achieve aims such as zero steady state error and fast dynamic response.

According to the AC side model of system shown in Figure 4, the AC current controller can be designed. Supposing the phase of grid voltage as reference phase, the direct component of current (i_d) is related to active power and quadratic component (i_q) is related to reactive power injected to grid. Considering coupling inductor with L_f = 2 mH in Figure 4, the bandwidth of current controller is set to 1 kHz where k_{Pi} = 0.1 and k_{Ii} = 16000.

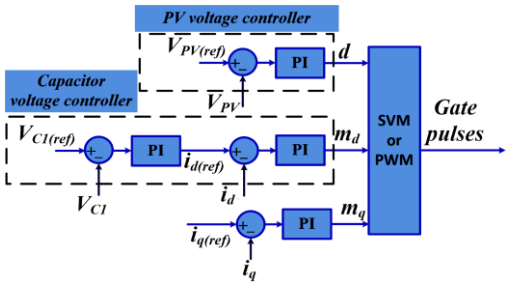

Figure 3. The proposed two stages controller

B. Capacitor Voltage Controller

The capacitor voltage controller provides current reference for AC current controller so that set the capacitor voltage to its reference. The proper operation of PWM algorithm is directly related to reference value for capacitor voltage. Because of single stage configuration of Γ-source inverter, the shoot through cycles must be replaced only among null vectors of (000) and (111) in PWM leaving active vectors unchanged. The following inequalities represent the conditions of proper switching in difference control method.

$$\begin{cases} M \le 1-D \xrightarrow{\text{for}} SBC \\ M \le \dfrac{2}{\sqrt{3}}(1-D) \xrightarrow{\text{for}} MCBC \\ M \le \left(2\pi / 3\sqrt{3}\right)(1-D) \xrightarrow{\text{for}} MBC \end{cases} \quad (18)$$

where, *SBC*, *MCBC* and *MBC* are simple boost control, maximum constant boost control and maximum boost control [9, 10].

According to Equations (6), (8) and (9) and considering Equation (18), the capacitor allowable voltage for proper operation of PWM is as:

$$\begin{cases} V_{C1} \ge 2V_{in} \xrightarrow{\text{for}} SBC \\ V_{C1} \ge \sqrt{3}V_{in} \xrightarrow{\text{for}} MCBC \\ V_{C1} \ge \dfrac{3\sqrt{3}}{\pi}V_{in} \xrightarrow{\text{for}} MBC \end{cases} \quad (19)$$

Regulating the capacitor voltage to a proper reference voltage make balance between PV power generating and injected power to grid. For example, when the PV power increases, its excessive energy that is not transferred to grid is stored in C_1 which increase its voltage higher than its reference. In this condition, the AC current controller must increase the active power injected to grid to subside capacitor voltage to its reference. Inversely, when PV power drops, the injected power to grid is become higher than PV power, which leads to decrease of capacitor voltage. When the capacitor voltage controller senses the drop in capacitor, it reduces the active power to grid to increase the capacitor voltage to its reference voltage.

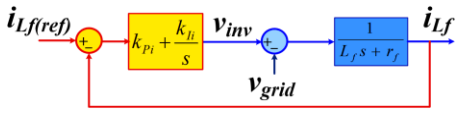

Figure 4. AC current controller model in Laplace domain

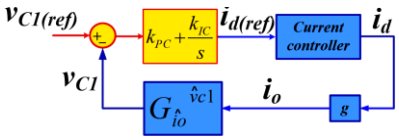

Figure 5. Capacitor voltage controller model in Laplace domain

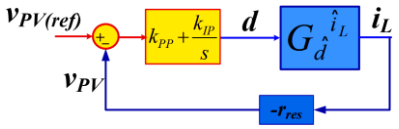

Figure 6. PV voltage controller model in Laplace domain

Achieving above mentioned requirements, the coefficients of capacitor controller must be negative. Since the capacitor voltage is related to active power exchange with grid, reference value for i_d must be generated in capacitor voltage controller while i_q is set to zero to eliminate reactive power exchange with grid. The capacitor voltage controller model in Laplace domain is shown in Figure 5.

In the Figure 5, i_o is related to i_d with coefficient of (g) which is a constant value in a certain modulation index and inverter shoot through duty cycle. According to the impedance network specification listed in Table 1, the bandwidth of capacitor voltage controller is set to 100 Hz with K_{PC} = -0.1 and K_{IC} = -20.

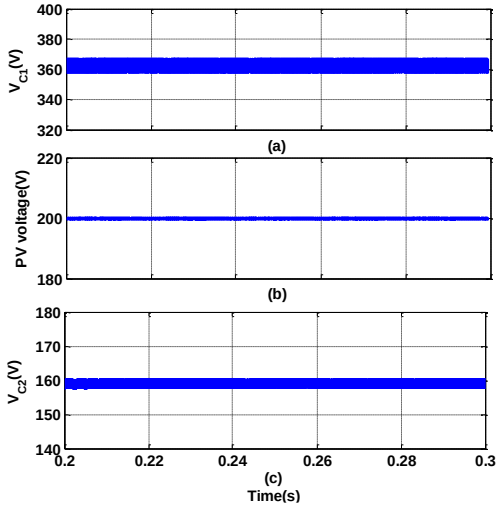

Figure 7. Voltages in steady state condition, (a) Capacitor voltage, (b) PV voltage

C. PV Voltage Controller

Setting capacitor voltage to its reference, the PV voltage controller can be designed with a specific bandwidth lower than capacitor voltage controller. The inverter shoot through duty cycle is due to regulate the PV voltage to its reference. The PV voltage controller model in Laplace domain is shown in Figure 6. In this figure, (r_{res}) significant the equivalent resistance of PV module around its operating point [16]. Considering the capacitor voltage regulated to its reference, increase in D lead to lowering the PV voltage and inversely PV voltage is increased when D is reduced.

Therefore, the PV voltage controller parameters must be negative. According to system parameters and supposing r_{res} = 4, the PV voltage controller is designed with bandwidth of 25 Hz where K_{PP} = -0.002 and K_{IP} = -0.1. As can be seen, the bandwidth of the PV voltage controller is lower than capacitor voltage controller, which discourage dynamic interactions between PV voltage, and capacitor voltage controller.

IV. SIMULATION RESULTS

Simulations are performed to verify the performance of the proposed controller and confirm our analysis. To this aim, a typical PV system based on asymmetrical Γ-source inverter as PEI system is simulated in MATLAB/Simulink environment. The system parameters and controller coefficients is the same presented in section III. The grid phase-null voltage is assumed to be 120 V(RMS) with frequency of 60 Hz. As shown in Figure 1, the proposed system is connected to the main grid through inductor of L_f as coupling impedance, which lowers the switching stress on inverter current.

The switching frequency of inverter leg is considered to be 10 kHz and the PWM algorithm is based on SBC which is a simple method of switching. Operation of PEI system and its controllers in impedance network side in steady state are investigated in Figure 1. Capacitor voltage controller is required to set capacitor voltage to 360 V, which is in allowable limit presented in Equation (19). Moreover, the PV voltage reference is set to 200 V to absorb maximum available power from PV system.

Table 1. The system parameters

Circuit parameters	Values
C_1 and C_2	400 µF
L	2 mH
L_m	400 µH
r_L	0.1 Ω
r_f	0.1 Ω
n	1.5
I_o	25 A
D	0.15

As can be seen in Figure 7(a), V_{C1} is equal to its reference of 360V with no steady state error. As known, the proper operation of the inverter-switching algorithm is directly related to the V_{C1}, which is set to a proper voltage stated in Equation (19). In Figure 7(b) the PV voltage is 200 V which is set to the reference provided by MPPT algorithm. As can be seen, the PV voltage controller sets the PV voltage to its reference without steady state error.

The proper operation of the PV voltage controller is directly related to proper operation of the V_{C1} controller. The capacitor "2" which its value is dependent to the PV voltage and capacitor "1" voltage and isn't set to a specific voltage is shown in Figure 7(c). As can be seen, the voltage across the capacitor "2" is much lower than capacitor "1" which is one of advantages of the utilizing the proposed converter as interface system for PV.

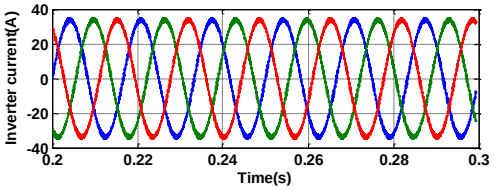

Figure 8. Inverter current

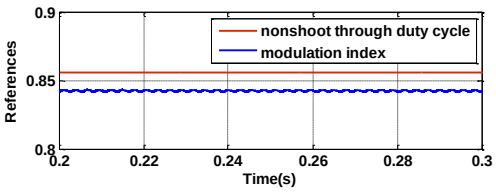

Figure 9. Reference signals in PWM algorithm

The inverter current in AC side in steady state condition is shown in Figure 8. As can be seen the inverter current has completely sinusoidal wave form which confirm the proper operation of the PWM algorithm. This is noted that the proper operation of PWM is dependent to choose of a suitable reference voltage for capacitor "1" in its allowable range.

The inverter modulation index and shoot through duty cycle is shown in Figure 9. According to Equation (18), for proper operation of switching algorithm, this is essential to modulation index be lower than inverter nonshoot through duty cycle which is (1-D) in Equation (18).

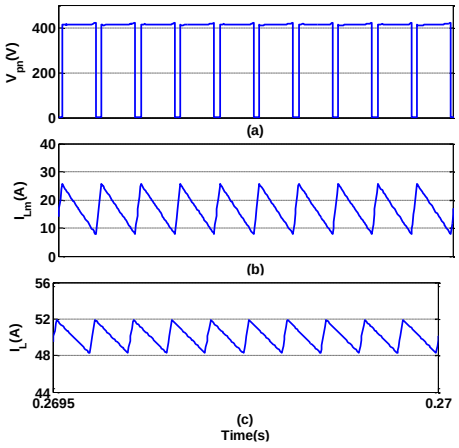

Figure 9. Switching process, (a) Inverter legs voltage, (b) Input inductor current (i_L), (c) Transformer magnetizing current (i_{Lm})

As can be seen in Figure 9, in steady state condition, the modulation index is always lower than nonshoot through duty cycle (i.e. M < 1-D) confirming the placement of shoot through cycles only between null vectors. The inverter voltage in DC side (v_{pn}) is shown in Figure 10(a). In shoot through cycles, v_{pn} is zero and in nonshoot through states, it reaches to about 410 V. During the shoot through condition, the energy stored in transformer and inductor in impedance network is increased while in nonshoot through condition these energies are released to capacitors. The current of magnetic components are shown in Figure 10(b) and (c).

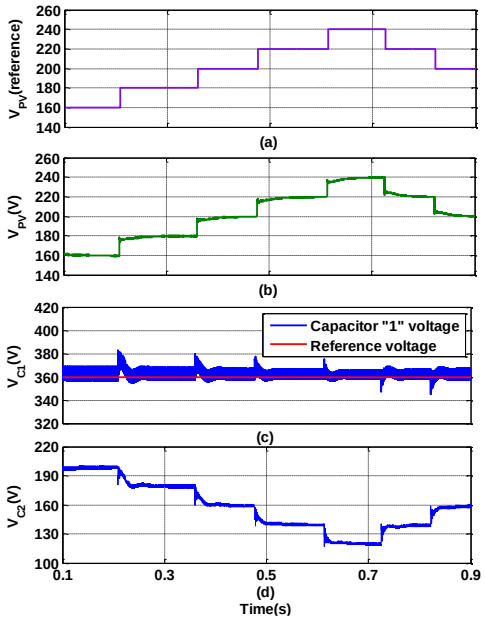

Figure 10. MPPT algorithm, (a) PV voltage reference, (b) PV voltage, (c) Capacitor "1" voltage, (d) Capacitor "2" voltage

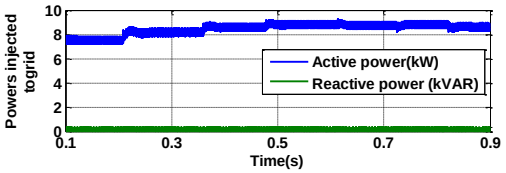

Figure 11. Injected powers to grid

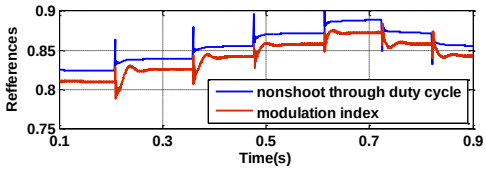

Figure 12. Reference signals in PWM

As can be seen the transformer magnetizing current and inductor current in impedance network side is increased in shoot through cycles and decreases in nonshoot through states releasing their energy to capacitors and load. The operation of the proposed two stages controller to change the PV voltage reference for finding its maximum power point is shown in Figure 11. The PV voltage reference is varied in some steps for finding maximum power point in the way shown in Figure 11(a).

The PV voltage responses to this step change of PV reference voltage are shown in Figure 11(b). As can be seen the PV voltage controller is able to fix PV voltage to its desired reference properly. As mentioned, the proper operation of the PV voltage controller is dependent to capacitor voltage controller performance, therefore this is important to capacitor "1" voltage be fixed in its reference voltage during PV voltage variations. The capacitor "1" voltage during PV voltage reference variations is shown in Figure 11(c). According to Figure 11(c), capacitor voltage is always regulated to its reference of 360 V.

The capacitor "2" voltage during PV voltage step changes is shown in Figure 11(d). Since capacitor "2" isn't equipped to a special controller, its voltage is a function of PV voltage and V_{C2}, therefore varies when PV voltage changes. The PV system powers injected to the main grid in AC side is shown in Figure 12. By variation of PV voltage, the injected active power to grid is varied in the way shown in Figure 12. As can be seen, when the PV voltage is about 220 V, the maximum power is injected to the grid. Since i_q is set to zero in AC side current controller, there is no reactive power exchange between the main grid and PV system.

As mentioned, the proper operation of the PWM algorithm and subsequently proper operation of whole system achieves when the modulation index and inverter shoot through duty cycle inequality in Equation (18) is performed. The inverter modulation index and inverter nonshoot through duty cycle is shown in Figure 13. Since the V_{C1} is regulated to a right value, the inverter modulation index is always lower than its nonshoot through duty cycle. The Figure 13 confirm the proper switching algorithm which in it, the shoot through cycles only occurs during null vectors leaving active vectors unchanged.

V. CONCLUSIONS

This paper has been presented the dynamic modeling of the Γ-source inverter that is a suitable converter for PV applications. Using the obtained dynamic model of the system, a two stages controller is designed to achieve requests such as proper switching algorithm, injecting power generated by PV to the main grid and maximum power point algorithm. In this control strategy, one of the capacitor voltages in impedance network side is regulated to its reference so that make balance between produced PV power and injected power to grid and ensure proper switching algorithm in PWM.

Keeping the capacitor voltage to its reference using adjustment of active component of AC current, the PV voltage controller can regulate PV voltage to its reference provided by MPPT controller. The performance of the two stages controller in regulating the capacitor voltage and PV voltage is verified by simulation results both in steady state and transient states. Moreover this has been shown that the proposed controller achieve proper operation of PWM algorithm which in it the shoot through cycles is placed only in null vectors.

REFERENCES

[1] F.Z. Peng, "Z-Source Inverter", IEEE Trans. Ind. Applicat., Vol. 39, pp. 504-510, Mar./Apr. 2003.

[2] F.Z. Peng, M.S. Shen, K. Holland, "Application of Z-Source Inverter for Traction Drive of Fuel Cell-Battery Hybrid Electric Vehicles", IEEE Trans. Power Electron., Vol. 22, No. 3, pp. 1054-1061, May 2007.

[3] J. Jung, A. Keyhani, "Control of a Fuel Cell Based Z-Source Converter", IEEE Trans. Ind. Electron., Vol. 22, No. 2, pp. 467-476, Jun. 2007.

[4] D. Cao, S. Jiang, X. Yu, F.Z. Peng, "Low-Cost Semi-Z-Source Inverter for Single-Phase Photovoltaic Systems", IEEE Trans. Power Electron., Vol. 26, No. 12, pp. 3514-3523, Dec. 2011.

[5] S. Zhang, K. Tseng, D.M. Vilathgamuwa, T.D. Nguyen, X. Wang, "Design of a Robust Grid Interface System for PMSG-Based Wind Turbine Generators", IEEE Trans. Ind. Electron., Vol. 58, No. 1, pp. 316-328, Jan. 2011.

[6] S.M. Dehghan, M. Mohamadian, A.Y. Varjani, "A New Variable-Speed Wind Energy Conversion System Using Permanent-Magnet Synchronous Generator and Z-Source Inverter", IEEE Trans. Energy Convers., Vol. 24, No. 3, pp. 714-724, Sep. 2009.

[7] Z.J. Zhou, X. Zhang, P. Xu, W.X. Shen, "Single-Phase Uninterruptible Power Supply Based on Z-Source Inverter", IEEE Trans. Ind. Electron., Vol. 55, No. 8, pp. 2997-3003, Aug. 2008.

[8] C.J. Gajanayake, D.M. Vilathgamuwa, P.C. Loh, R. Teodorescu, F. Blaabjerg, "Z-Source-Inverter-Based Flexible Distributed Generation System Solution for Grid Power Quality Improvement", IEEE Trans. Energy Convers., Vol. 24, No. 3, pp. 695-704, Sep. 2009.

[9] F.Z. Peng, M. Shen, Z. Qian, "Maximum Boost Control of the Z-Source Inverter", IEEE Trans. Power Electron., Vol. 20, No. 4, pp. 833-838, Jul./Aug. 2005.

[10] M. Shen, J. Wang, A. Joseph, F.Z. Peng, "Constant Boost Control of the Z-Source Inverter to Minimize Current Ripple and Voltage Stress", IEEE Trans. Ind. Applicat., Vol. 42, No. 3, pp. 770-778, May/June 2006.
[11] M. Zhu, K. Yu, F.L. Luo, "Switched Inductor Z-Source Inverter", IEEE Trans. Power Electron., Vol. 25, No. 8, pp. 2150-2158, Aug. 2010.
[12] W. Qian, F.Z. Peng, H. Cha, "Trans-Z-Source Inverters", IEEE Trans. Power Electron., Vol. 26, No. 12, pp. 3453-3463, Dec. 2011.
[13] M.K. Nguyen, Y.C. Lim, Y.G. Kim "TZ-Source Inverters", IEEE Trans. Ind. Electron., Vol. 60, No. 12, pp. 5686-5695, Dec. 2013.
[14] W. Mo, P.C. Loh, F. Blaabjerg, "Asymmetrical Γ-Source Inverters", IEEE Trans. Ind. Electron., Vol. 61, No. 2, pp. 637-647, Feb. 2014.
[15] H. Hosseini, M. Farsadi, A. Lak, H. Ghahramani, N. Razmjooy, "A Novel Method Using Imperialist Competitive Algorithm (ICA) for Controlling Pitch Angle in Hybrid Wind and PV Array Energy Production System", International Journal on Technical and Physical Problems of Engineering (IJTPE), Issue 11, Vol. 4, No. 2, pp. 145-152, June 2012.
[16] S. Nema, R.K. Nema, G. Agnihotri, "MATLAB/Simulink Based Study of Photovoltaic Cells/Modules/Array and their Experimental Verification", International Journal of Energy and Environment, Vol. 1, Issue 3, pp. 487-500, 2010.

BIOGRAPHIES

Farzad Khoshkhati received the B.Sc. degree in Electrical Engineering from University of Zanjan, Zanjan, Iran (2006-2011) and M.Sc. degree in Mechatronics from University of Tehran, Tehran, Iran (2011-2013).

Siroos Toofan received the B.Sc. degree in Electronics Engineering from Amirkabir University of Technology (Tehran Polytechnic), Tehran, Iran in 1999, and the M.Sc. and Ph.D. degrees in Electronics Engineering form Iran University of Science and Technology, Tehran, Iran in 2002 and 2008, respectively. From 2007 to 2008, on his sabbatical leave, he was with the VLSI group of Politechnico di Torino and in the Microelectronics Integrated Circuits Lab. of the Politechnico di Milano Universities in Italy. He has been working as Assistant Professor with the Department of Electrical Engineering, University of Zanjan, Zanjan, Iran since 2009. His current research activities include the design of CMOS analog integrated circuits, RF integrated circuits, capacitive sensors readout circuits and energy harvesting circuits.

Behzad Asaei received the B.Sc. and M.Sc. degrees from the University of Tehran, Tehran, Iran, in 1988 and 1990, respectively, and the Ph.D. degree from the Sydney University, NSW, Australia, in 1995, all in Electrical Engineering. Since 2006, he has been the Director of the Energy and Automotive Technology Laboratory, School of Electrical and Computer Engineering, University of Tehran, Tehran, Iran. His research interests include the field of automotive electronics, solar energy, electric and hybrid electric vehicles, power electronics, and motor drives in which several projects including two electric vehicles, hybrid electric locomotive, solar car, hybrid motorcycle, electric bike, and automotive electronics are completed.